Cancer Chemother Pharmacol (2012) 69:155–164
DOI 10.1007/s00280-011-1662-4

ORIGINAL ARTICLE

Further characterisation of the cellular activity of the DNA-PK inhibitor, NU7441, reveals potential cross-talk with homologous recombination

Michele Tavecchio · Joanne M. Munck · Celine Cano · David R. Newell · Nicola J. Curtin

Received: 9 August 2010 / Accepted: 19 April 2011 / Published online: 1 June 2011

Abstract
Purpose Inhibition of DNA repair is emerging as a new therapeutic strategy for cancer treatment. One promising target is DNA-PK, a pivotal kinase in double-strand break repair. The purpose of this study was to further characterise the activity of the DNA-PK inhibitor NU7441, giving some new insights into the biology of DNA-PK.
Methods We used NU7441, a potent DNA-PK inhibitor, to evaluate potential pharmacodynamic markers of DNA-PK inhibition, inhibition of DNA repair and chemo- and radio-potentiation in isogenic human cancer cells proficient (M059-Fus1) and deficient (M059 J) in DNA-PK.
Results NU7441 strongly inhibited DNA-PK in cell lines (IC_{50} = 0.3 μM) but only weakly inhibited PI3 K (IC_{50} = 7 μM). The only available anti-phospho-DNA-PK antibody also recognised some phosphoprotein targets of ATM. NU7441 caused doxorubicin- and IR-induced DNA DSBs (measured by γ-H2AX foci) to persist and also slightly decreased homologous recombination activity, as assessed by Rad51 foci. Chemo- and radio-potentiation were induced by NU7441 in M059-Fus-1, but not in DNA-PK-deficient M059 J cells. DNA-PK was highly expressed in a chronic lymphocytic leukaemia sample but undetectable in resting normal human lymphocytes, although it could be induced by PHA-P treatment. In K652 cells, DNA-PK expression was not related to cell cycle phase.
Conclusion These data confirm NU7441 not only as a potent chemo- and radio-sensitiser clinical candidate but also as a powerful tool to study the biology of DNA-PK.

Keywords DNA-PK · NU7441 · Chemo- and radio-potentiation · γ-H2AX · Rad51 · HR

M. Tavecchio · J. M. Munck · C. Cano · D. R. Newell · N. J. Curtin (✉)
Northern Institute for Cancer Research,
School of Medical Sciences, Newcastle University,
Paul O' Gorman Building, Framlington Place,
NE2 4HH Newcastle upon Tyne, UK
e-mail: n.j.curtin@newcastle.ac.uk

Introduction

DNA is the principal target of many conventional anticancer agents, and inhibition of DNA repair is one of the most promising strategies in modern cancer therapy. Many DNA repair inhibitors are entering clinical trials, both in combination with genotoxic agents and alone. Of particular interest are the inhibitors of DNA double-strand break (DSB) repair pathways, as DSBs are considered exceptionally lethal DNA lesions, with a single unrepaired DSB potentially able to kill the cell [1]. To repair DSBs, two major mechanisms have evolved: homologous recombination (HR) and non-homologous end joining (NHEJ). HR is error-free, depending on the presence of sister chromatids to provide a DNA template identical to the damaged one, and therefore, it is active only in late S and G_2 phases of the cell cycle. NHEJ does not require a template and, although error-prone, it is active throughout the cell cycle. NHEJ is therefore an attractive target for the sensitisation of cancer cells in every phase of the cell cycle to DSB-inducing agents, such as ionising radiation (IR) and topoisomerase II (topo II) poisons, used in cancer therapy. Among factors involved in NHEJ, DNA-PK is now gaining interest as a key protein in the process.

The catalytic subunit (DNA-PKcs) is a serine–threonine kinase whose gene is located on human chromosome 8. DNA-PK is a member of the PI3 kinase-like kinase (PIKK)

family along with ATM and ATR and functions as a trimer with Ku70 and Ku86. Following DSB induction, the Ku heterodimers, followed by DNA-PKcs, bind to the DNA termini. This results in a series of phosphorylation events, including the DNA-PK-specific autophosphorylation of serine 2056 [2], which is therefore a good indicator of DNA-PK activation. The series of phosphorylations allows the recruitment of other NHEJ factors such as exonucleases (Xrcc4, Artemis), polymerases and ligases (Ligase IV, XLF/Cernunnos) that resect or fill in the DNA termini until they are paired and eventually ligated [3].

NHEJ is fundamental in DSB repair and in immune system development for V(D)J recombination [4]. Mice deficient for DNA-PK are SCID (severe combined immune deficient) and fail to produce mature T and B lymphocytes, but are viable and fertile [5]. DNA-PK also has a role in the phosphorylation and control of many cell cycle proteins [6], and in human cell lines depleted of ATM, DNA-PK is responsible for the activation of a G2 checkpoint after IR [7].

In clinical settings, DNA-PK has been implicated in resistance to nitrogen mustards [8] and is an attractive target in chronic lymphocytic leukaemia (CLL) patients, in particular those where a del(17p) or a del(11q) genotype is observed [9].

NU7441 (2-N-morpholino-8-dibenzothiophenyl-chromen-4-one) is a potent (IC_{50} = 12 nM) ATP-competitive DNA-PK inhibitor developed from the PI3 K inhibitor LY294002 [10]. Previous combination studies with topoisomerase II poisons and IR demonstrated its activity in cell lines irrespective of p53 status and also in SW620 tumour-bearing mice [11].

Here, we report the further characterisation of NU7441 and show, in isogenically paired DNA-PKcs-proficient and DNA-PKcs-deficient human cancer cell lines, that chemo- and radio-potentiation are only observed in DNA-PK-proficient cells, along with the persistence of DSBs and inhibition of HR. Inhibition of repair was related to the inhibition of DNA-PKcs autophosphorylation and not inhibition of PI3 K, a potential off-target effect of DNA-PK inhibitors. In order to develop a possible biomarker, DNA-PK expression was studied in potential surrogate normal tissue but was undetectable in resting lymphocytes from healthy volunteers compared to a CLL sample and to a human tumour xenograft.

Materials and methods

Chemicals

All chemicals were obtained from Sigma (Poole, UK) unless stated otherwise. NU7441 was synthesised as previously described [10] and was dissolved at 2 mM in DMSO. KU-55933 (Dr. Graeme Smith, AstraZeneca, Alderley Park, UK) was dissolved at 20 mM in DMSO, and ZSTK474 was synthesised as previously described [12] and was dissolved at 10 mM in DMSO. Doxorubicin was dissolved in PBS at 1 mM, phytohemagglutinin-P (PHA-P) was dissolved in water, and IGF (insulin-like growth factor) was purchased from Calbiochem (USA). All solutions were kept at −20°C, and neocarzinostatin (NCS) was stored at 4°C in the dark.

Cell lines

Glioblastoma cell lines M059 J (DNA-PK−/−) [13] and M059-Fus-1 (transfected with extra copies of chromosome 8, bearing the DNA-PK gene) were grown in DMEM + 10% (v/v) heat-inactivated FBS, 1% (w/v) glutamine, penicillin (50 units/ml) and streptomycin (50 μg/ml). M059-Fus-1 cells were cultured in the presence of 200 μg/ml of G418 (Gibco) to retain the extra copies of chromosome 8. K562 and SW620 cells were maintained in RPMI-1640 plus 10% (v/v) FBS, 1% (w/v) glutamine, penicillin (50 units/ml) and streptomycin (50 μg/ml). All cells lines were maintained at 37°C in a 5% CO_2 atmosphere and were *Mycoplasma* free and used when under the 30th passage.

Elutriation

About 6×10^8 K562 cells were run in a centrifugal elutriator (Avanti J-20P, Beckman Coulter, USA) at 1,200 rpm and collected, based on their different sizes, to obtain populations in the different cell cycle phases. An aliquot of every fraction was taken for DNA content measurement, to assess the cell cycle phase.

Cytotoxicity studies

Clonogenic assays were performed by pre-treating cells with or without NU7441 (1 μM) for 1 h and then co-incubating them with doxorubicin for 24 h or X-irradiation (0.35 Gy/min, Gulmay Medical Ltd., Camberly, UK) and a further 24-h incubation with NU7441. Cells were then trypsinised, seeded into 10-cm Petri dishes at the desired density, allowed to form colonies for 14 days, then stained with crystal violet and quantified with an automated colony counter (ColCount, Oxford Optronics Ltd., Oxford, UK). The survival reduction factor (SRF) was calculated by dividing the percentage survival of cells treated with cytotoxic agent alone by the percentage survival of cells treated with cytotoxic plus NU7441.

γ-H2AX and Rad51 foci

γ-H2AX, the phosphorylated form of a histone variant protein that is a marker of DSBs [14] and Rad51 foci, indicative

of HR, were detected by immunofluorescence. Briefly, cells were seeded on coverslips, treated with 2 Gy IR with or without 1 h pre-treatment with 1 μM NU7441. At different time points after irradiation, coverslips were fixed with −20°C methanol for 15 min, rehydrated with KCM buffer [11], blocked with KCM buffer plus 10% (w/v) milk and 2% (w/v) BSA and then incubated overnight with primary antibodies (1/1,000 for anti-γ-H2AX, code 05-636, Millipore, Watford, UK and 1/200 for anti-Rad51, code sc-8349, Santa Cruz Biotechnology, Santa Cruz, CA, USA). After three washes with wash buffer (KCM buffer plus 0.1% (v/v) Triton X-100), cells were incubated for 1 h with secondary antibodies (Alexa Fluor 488, Invitrogen, UK), washed again and mounted with DAPI (4′,6-diamidino-2-phenylindole)-containing Vectashield (Vector Laboratories, Burlingame, CA). Images were acquired as previously shown [11] and analysed by ImageJ software (NIH, Bethesda, MD, USA) with at least 70 cells/field counted.

Animal studies

All in vivo experiments were reviewed and approved by the relevant institutional animal welfare committee and performed according to national law. C57 Balb/C nude mice were implanted s.c. with 10^7 SW620 cells. When tumours were palpable, mice were untreated ($t = 0$) or treated with 20 mg/kg of doxorubicin and killed at 0, 1 and 24 h, and tumours were removed and snap-frozen. Before protein extraction, tumours were ground in liquid nitrogen and treated with Red Blood Cell Lysis Solution (Qiagen, Maryland, USA) to remove blood cells.

Preparation of peripheral blood mononuclear cells (PBMCs)

For CLL sample and healthy human lymphocyte collection, informed consent was obtained and the study was carried out under national ethical guidelines. Five millilitres of blood from healthy donors was put in Nycomed Lymphoprep (Axis-Shield, Oslo, Norway), centrifuged and washed with PBS. Lymphocytes were then frozen at −80°C until protein extraction or transferred to culture flasks with 5 ml of RPMI-1640 plus 10% (v/v) FBS, 1% (w/v) glutamine, penicillin (50 units/ml) and streptomycin (50 μg/ml) and different concentrations of PHA-P for 72 h. DNA content was measured to assess the replicative state of lymphocytes: an aliquot of every fresh or cultured lymphocyte sample was taken and fixed with 70% (v/v) ethanol at −20°C for 4 h, stained overnight at 4°C with 2.5 μg/ml of propidium iodide and analysed with a FACSscan flow cytometer (Becton–Dickinson, UK) for DNA content. Analyses were performed by CellQuest software (Becton–Dickinson, UK). For pSer2056-DNA-PK detection, 5 ml of blood were treated for 20 min with 10 nM of NCS, then lymphocytes prepared and protein extracted.

Protein extraction and western blotting

Cell pellets were treated with an ice-cold solution (250 mM Tris–HCl, 40% (v/v) glycerol and 5% (w/v) SDS or Phosphosafe Extraction Reagent, Merck, UK) with protease inhibitor (code 11873580001, Roche, UK) and phosphatase inhibitors (codes P2850 and P5726, from Sigma) and then sonicated for 20 s to disrupt DNA, centrifuged and supernatants kept at −80°C until protein quantification. Gel electrophoresis was carried out with 3–8% (w/v) Tris–Acetate XT-Criterion Gels (Biorad, UK), and blotting was performed on nitrocellulose membrane (Hybond C extra, Amersham Biosciences, UK). After 1 h blocking (PBS-T with 5% (w/v) BSA for phosphorylated proteins or milk for total proteins) and 4°C overnight incubation with primary antibodies: mouse monoclonal anti-actin, code A1978 (Calbiochem, Merck Biosciences, Nottingham, UK), anti-rabbit polyclonal anti-pSer2056DNA-PKcs, code Ab18192 (Abcam Cambridge, UK), rabbit polyclonal anti-total DNA-PKcs, code sc-9051 (Santa Cruz Biotechnology), rabbit monoclonal anti-pSer345-Chk1, code 2348 (New England Biolabs, Hitchin, UK), mouse monoclonal anti-Chk1, code sc-8408 (Santa Cruz Biotechnology, Santa Cruz, CA), rabbit monoclonal anti-pSer1981-ATM, code AF1655 (R&D Systems, Abingdon, UK), mouse monoclonal anti-ATM, code A1106 (Sigma, Poole, UK), rabbit monoclonal anti-pAKT and anti-total AKT, codes 4058 and 4691 (New England Biolabs, Hitchin, UK), membranes were washed in PBS-T, incubated with HRP-conjugated secondary antibodies (goat anti-mouse, code P0447 and goat anti-rabbit, code P0448, Dako, Ely, UK) and visualised using ECL. Images were acquired by means of the Fuji LAS 3000 (Raytek, Sheffield, UK) and analysed by Aida Image Analyzer.

Statistical analysis

Data were not weighted, and IC_{50} values for cellular DNA-PK inhibition were calculated by plotting the mean values and fitting a sigmoidal dose–response curve by least square regression analysis. IC_{50} value for PI3 K inhibition was calculated by plotting the mean pAKT values and fitting a polynomial function of second order.

Data were analysed by Microsoft Excel and GraphPad Prism software (GraphPad Software, Inc., San Diego, CA). Significant differences were determined by a two-tailed unpaired t test.

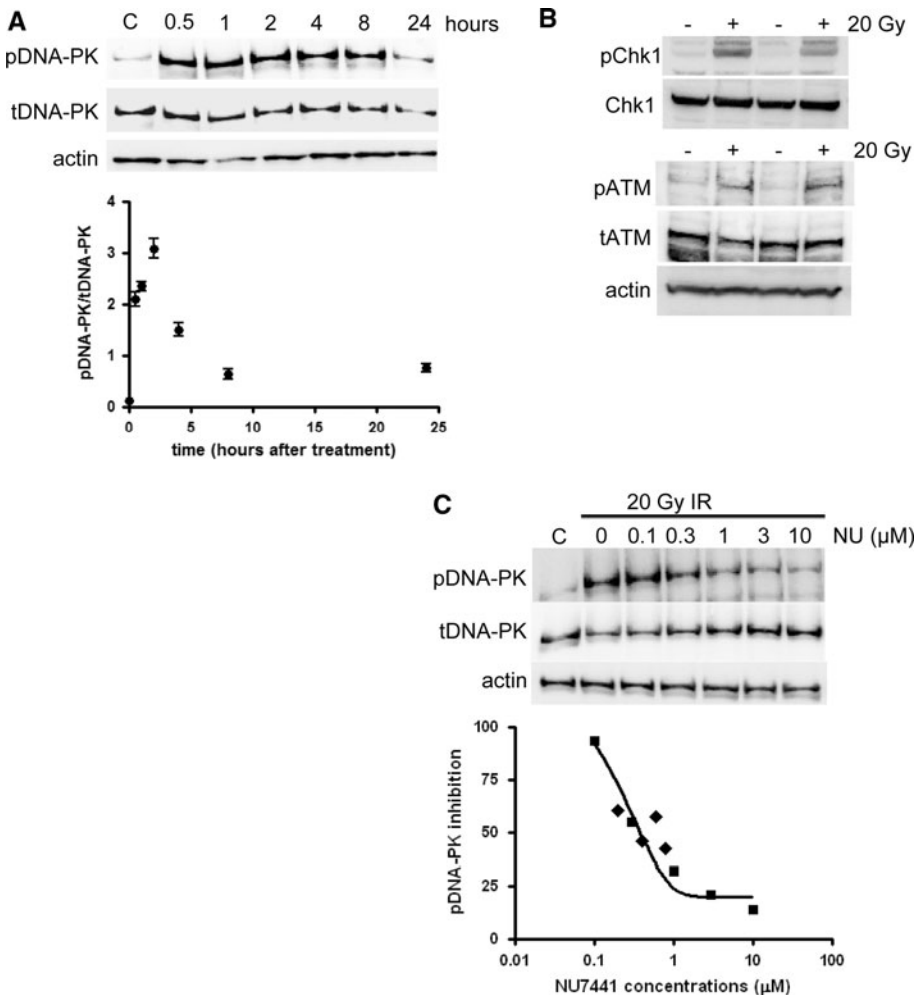

Fig. 1 DNA-PK is activated by DSB-inducing agents and is inhibited by NU7441. **a** Induction of DNA-PK autophosphorylation in response to IR. K562 cells were irradiated with 20 Gy IR, proteins extracted at different time points and 10 μg were analysed. Shown are representative Western blots from three independent experiments for phospho- and total DNA-PK, and a *graph* displaying the data expressed as the mean pS2056-DNA-PK:total DNA-PK ratio ± SD. **b** Induction of ATM (Ser1981) and Chk1 (Ser345) phosphorylation in response to IR. K562 cells were exposed to 20 Gy IR. Following a 30-min incubation, cell lysates were prepared and 60 μg analysed by western blot. Representative data from two independent experiments are shown. **c** NU7441 is a potent inhibitor of DNA-PK in intact cells. K562 cells were pre-treated with different concentrations of NU7441, irradiated at 20 Gy and protein extracted. 25 μg of proteins were analysed. Shown are representative Western blots from two independent experiments and a *graph* of the combined data. Each *square* is the mean of two independent replicates, and *diamonds* are points from an additional experiment. The *line* is a sigmoidal dose–response curve fitted to the data

Results

Cellular activity and specificity of NU7441

To determine DNA-PK activity and inhibition in intact cells, we measured DNA-PK-specific autophosphorylation at serine 2056. In addition, because of the structural similarity between PI3 K and DNA-PKcs, and because NU7441 was developed from the PI3 K inhibitor LY294002, it was important to determine whether NU7441 inhibited PI3 K-dependent AKT phosphorylation on serine 473. Human chronic myelogenous leukaemia K562 cells have been used previously to determine the effects of DNA-PK inhibitors [15], and we therefore selected this cell line for investigation. DNA-PKcs autophosphorylation at Ser2056 was observed in K562 cells following DSB induction by 20 Gy (Fig. 1a). After IR, pSer2056-DNA-PK was detected at 30 min, with the highest levels reached at 2 h (Fig. 1a). From 2 h onwards, there was a decline in the phosphoprotein signal, indicating the decrease in DNA-PK activation. ATR-dependent phosphorylation of Chk1-Ser345 [16] and ATM autophosphorylation at Ser1981 [17] were also increased following exposure of K562 cells to 20 Gy IR (Fig. 1b).

NU7441 inhibited DNA-PK activity after IR stimulation in K562 cells in a concentration-dependent manner with a

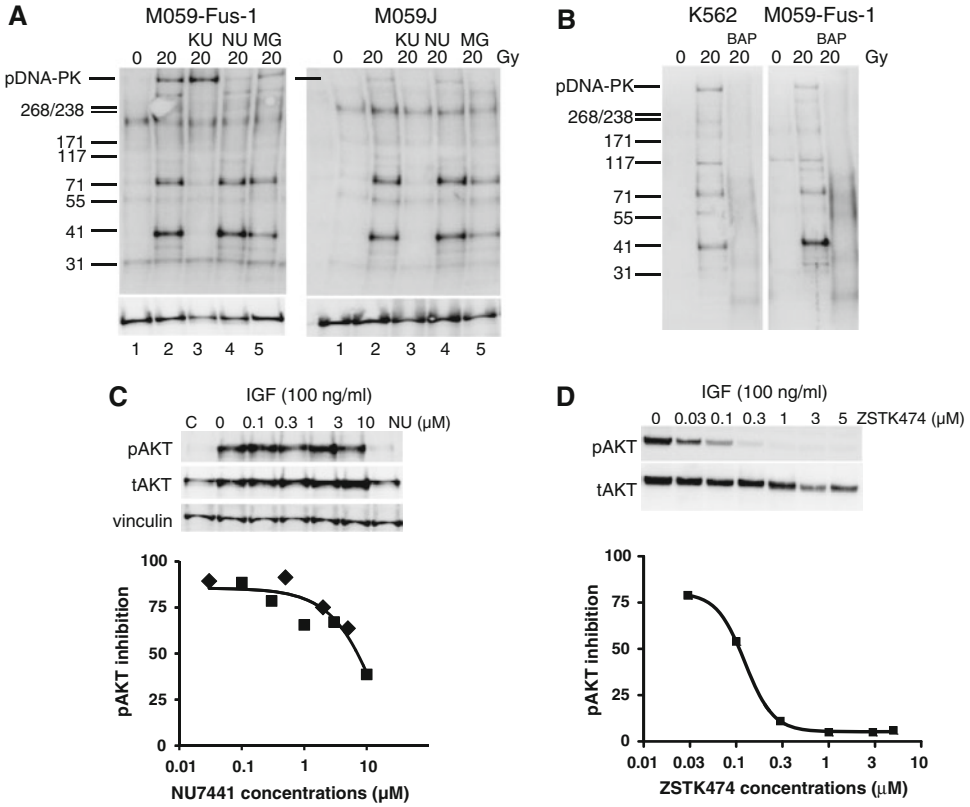

Fig. 2 An anti-pSer2056-DNA-PK antibody reveals DSB-induced phosphoproteins under the control of ATM, and NU7441 is a weak PI3 K inhibitor in cellular assays. **a** Following IR, several bands are detected by the anti-pSer2056-DNA-PK antibody as well as pSer2056-DNA-PK. These bands were apparent in both M069-Fus-1 cells (*left panel*) and M059 J cells (*right panel*). The additional bands detected by the anti-pSer2056-DNA-PK antibody were not DNA-PKcs degradation products because a proteasome inhibitor (MG132) did not prevent their appearance and because they were also detectable in M059 J cell extracts. NU7441 inhibits the appearance of pSer2056-DNA-PK but not the other bands, which are eliminated in the presence of the ATM inhibitor, KU55933. M059-Fus-1 or M059 J cells were treated with 10 μM KU-55933 or 1 μM NU7441 for 1 h, or 25 μM MG132 for 5 h, irradiated with 20 Gy, and after 30 min, proteins were extracted and 20 μg of proteins were analysed. *KU*, *NU* and *MG* indicate incubation with 10 μM KU55933, 1 μM NU7441 or 25 μM MG132, respectively, prior to the 20 Gy irradiation. Representative Western blot from two independent experiments are shown. **b** The bands recognised by the anti-pSer2056-DNA-PK antibody were phosphoproteins as demonstrated by the lack of signal following bovine alkaline phosphatase (BAP) treatment. Extracts from K562 and M059-Fus-1 cells were incubated at 37°C with 10 U of bovine alkaline phosphatase for 30 min and 20 μg of proteins was analysed. Representative Western blots from two independent experiments are shown. **c** NU7441 only inhibits AKT phosphorylation at >1 μM in a cell-based assay. K562 were treated for 30 min with 100 ng/ml of IGF ± increasing concentrations of NU7441, protein extracted and 50 μg of proteins analysed. Each *square* is the mean of two independent replicates, *diamonds* are points from an additional experiment. The *line* is a second-order polynomial function fitted to the data. **d** K562 cells were treated with increasing concentrations of ZSTK474 for 1 h, prior to a 30-min incubation with 100 ng/ml IGF-1. Cell lysates were prepared and 50 μg total protein analysed. The *graph* displays the data expressed as the ratio of pS2056-DNA-PK:total DNA-PK with a sigmoidal dose–response *curve* fitted to the data. Data are representative of two independent experiments

calculated IC_{50} of 0.3 μM (Fig. 1c). Studies in DNA-PK-deficient M059 J and DNA-PK-proficient M059-Fus-1, K562 and SW620 cells showed that pSer2056-DNA-PK was only detectable in DNA-PK-proficient cells (Fig. 2a compare left vs. right panel). However, in addition to pSer2056-DNA-PK, several non-specific bands were recognised by the antibody used. These additional bands only appeared after DSB induction (Fig. 2a lane 2 each panel), and in an IR dose-dependent fashion (data not shown), and were unlikely to be degradation products of DNA-PK as treatment with a proteasome inhibitor [18, 19] had no effect (Fig. 2a, lane 5 each panel). The disappearance of the bands after treatment with alkaline phosphatase revealed that they were phosphorylated proteins (Fig. 2b, compare lanes 2 and 3 each panel). Interestingly, the bands were also present in DNA-PK-deficient M059 J cells. Since ATM kinase also catalyses DNA-damage-induced phosphorylation events, we investigated the effect of the ATM inhibitor KU-55933 [20] on the formation of the bands. Most of the bands were undetectable in cells co-treated for 1 h with 10 μM KU-55933, suggesting that they were ATM-dependent phosphorylation events (Figs. 2a, lane 3 each panel).

As there is structural similarity in the kinase domains of DNA-PKcs and PI3 K, and because NU7441 was developed

from the PI3 K inhibitor LY294002, we investigated the specificity of NU7441 for DNA-PK over PI3 K in intact cells. Levels of pSer473-AKT increase after 30 min of IGF-1 stimulation (100 ng/ml) of PI3 K activity [21], as shown in Fig. 2c. NU7441 only inhibited IGF-stimulated AKT phosphorylation at Ser473 (basal expression was not inhibited, data not shown) at >1 μM, with a calculated IC_{50} of 7 μM, i.e. 20-fold selectivity compared to inhibition of DNA-PK. At the concentrations used (1 μM) in subsequent experiments, NU7441 did not substantially inhibit PI3 K. In a control experiment, we used the PI-3 K inhibitor ZSTK474 [2-(2-difluoromethylbenzimidazol-1-yl)-4,6-dimorpholino-1,3,5-triazine] [12] to confirm that it is possible to inhibit PI-3 K-dependent AKT phosphorylation in K562 cells and the IC_{50} value for the inhibition of cellular PI3 K activity by ZSTK474 was 0.1 μM (Fig. 2d).

In vitro chemo- and radio-potentiation by NU7441

We further investigated the cellular selectivity of NU7441 by determining radio- and chemo-sensitisation in isogenically paired DNA-PK-proficient M059-Fus-1 and DNA-PK-deficient M059 J human tumour cells. As expected, M059 J cells were more sensitive to DSB-inducing agents than M059-Fus-1 cells: following exposure to 100 nM doxorubicin survival in M059-Fus-1 cells was 25%, compared with only 1.4% in M059 J cells, while survival after 4 Gy IR was 34% in M059-Fus-1 cells and 8% in M059 J cells (Fig. 3a, b). The cloning potential (plating efficiency) of both cell lines was low (M059-Fus-1 = 4.4 ± 2.1% and M059 J = 3.4 ± 0.7%), but it was unaffected by 1 μM NU7441 (M059-Fus-1 = 4.3 ± 1.3% and M059 J = 3.7 ± 0.6%). NU7441 potentiated the cytotoxicity of doxorubicin by 3.5-fold and IR by twofold in M059-Fus-1 cells (Fig. 3a, b; Table 1). In the DNA-PKcs-deficient M059 J cells, NU7441 did not potentiate either IR or doxorubicin, demonstrating that the chemo- and radio-sensitisation by NU7441 in human cells is dependent on the presence of DNA-PK.

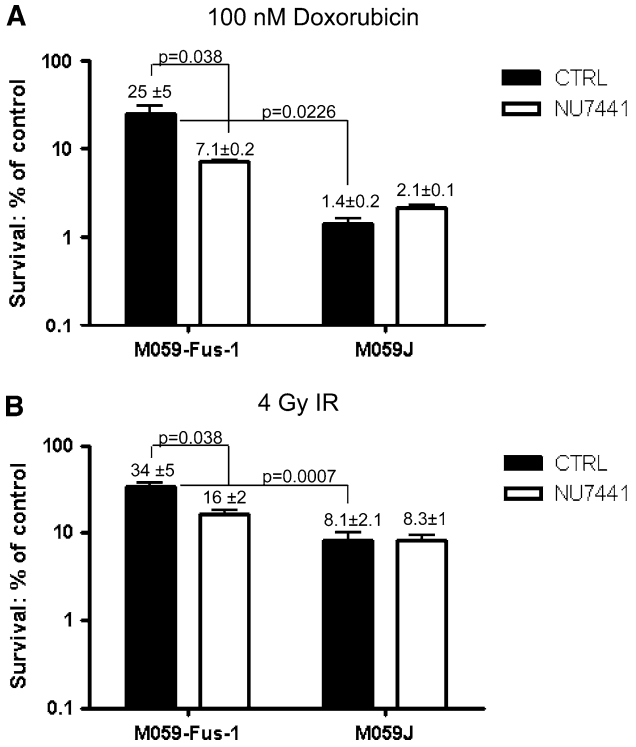

Fig. 3 NU7441 is a chemo- and radio-sensitiser only in DNA-PK-proficient cells. **a** Clonogenic survival of M059 J and M059-Fus-1 cells treated with 1 μM NU7441 or DMSO (control) for 1 h prior to doxorubicin co-treatment for 24 h. Data are the mean and standard deviation of three independent experiments, each in triplicate. **b** Clonogenic survival of M059 J and M059-Fus-1 cells treated with 1 μM NU7441 or DMSO (control) for 1 h prior to irradiation and a further 24 h incubation. Data are the mean and standard deviation of three independent experiments, each in triplicate

NU7441 retards DSBs repair and inhibits HR

To confirm that the chemo- and radio-sensitisation conferred by NU7441 was due to an effect on DNA DSB repair, we followed the kinetics of γ-H2AX foci formation and dissolution after irradiation (4 Gy) by immunofluorescence microscopy. As shown in Fig. 4a, after irradiation,

Table 1 Effect of NU7441 on the cytotoxicity of ionising radiation and doxorubicin in DNA-PK-proficient and DNA-PK-deficient cells

	M059-Fus-1 (DNA-PK+)		M059 J (DNA-PK−)	
	Cytotoxic alone	Cytotoxic + NU7441	Cytotoxic alone	Cytotoxic + NU7441
IR LC_{50} Gy	1.7 ± 0.3	$0.72 \pm 0.23^{P=0.011}$	0.43 ± 0.21	0.38 ± 0.13^{ns}
IR LC_{90} Gy	7.0 ± 1.5	$3.4 \pm 1.0^{P=0.025}$	1.8 ± 0.3	1.9 ± 0.5^{ns}
Doxorubicin LC_{50} nM	57 ± 10	$16 \pm 4^{P=0.003}$	3.6 ± 0.9	3.1 ± 0.6^{ns}
Doxorubicin LC_{90} nM	203 ± 19	$78 \pm 12^{P=0.001}$	14 ± 4	12 ± 3^{ns}

LC_{50} and LC_{90} values calculated from dose response curves in M059-Fus-1 and M059 J cells treated with increasing doses of IR or concentrations of doxorubicin for 24 h, from at least 3 independent experiments. Significant differences in survival of cells co-treated with NU7441 versus cells treated with IR or doxorubicin alone (*P* values) are given as superscript

ns not significant

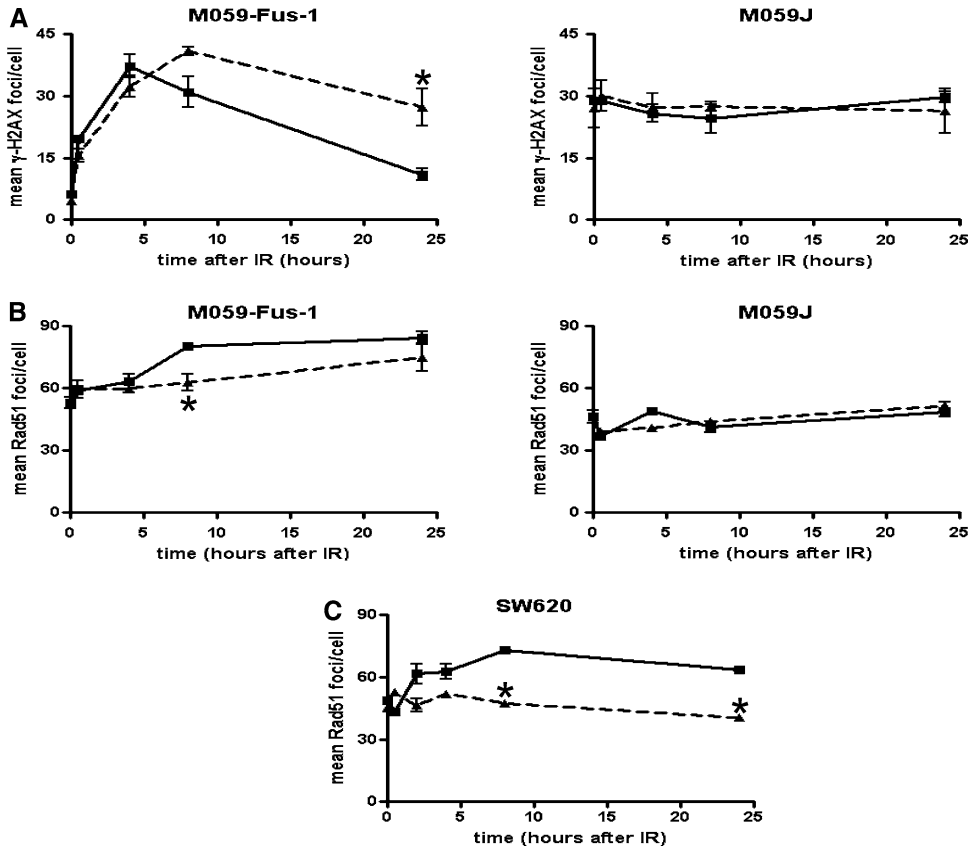

Fig. 4 NU7441 retards the repair of IR-induced DSBs and inhibits HR in a DNA-PK-dependent manner. **a**, **b** 24-h time course for γ-H2AX (**a**) and Rad51 (**b**) foci after 4 Gy irradiation in the presence of 1 μM NU7441 (*dashed line*) or DMSO (control, *solid line*). *Left* DNA-PK-proficient M059-Fus-1 cells, *right* DNA-PK-deficient M059 J cells. Data are the mean of four replicates, with 70 cells counted *per* replicate. Mean values and standard deviation are shown. **c** NU7441 inhibits HR in SW620 cells: 24 h time course of Rad51 foci after 4 Gy irradiation in the presence of 1 μM NU7441 (*dashed line*) or DMSO (control, *solid line*). Data are the mean of four replicates, with 70 cells counted *per* replicate. Mean plus standard deviation are shown. Asterisk indicates a statistically significant difference ($P < 0.05$)

there is an increase in the number of γ-H2AX foci in M059-Fus-1 cells, indicating the induction of DSBs. The foci disappear with time, such that at 24 h the number of foci was not significantly different from baseline, indicating that repair was essentially complete. There was no detectable induction of γ-H2AX foci by either IR or doxorubicin in M059 J cells although these cells had apparently high levels of baseline γ-H2AX focus formation, possibly reflecting induction of other H2AX kinases in response to persistent endogenous DSB. NU7441 treatment of M059-Fus-1 cells resulted in the persistence of γ-H2AX foci after IR (P value < 0.05 at 24 h relative to IR alone), indicating a delay in the repair due to DNA-PK inhibition. There was no effect of NU7441 on γ-H2AX foci levels in DNA-PK-deficient M059 J cells.

We also assessed the impact of NU7441 on HR as measured by Rad51 foci formation. During HR, the protein Rad51 forms a nucleoprotein filament that facilitates strand invasion, and therefore, detection of Rad51 foci can be used to evaluate HR activity. As shown in Fig. 4b, Rad51 foci accumulated in M059-Fus-1 cells after IR, peaking at 8 h, as γ-H2AX declines ($P < 0.05$). Interestingly, NU7441 inhibited the increase in Rad51 foci ($P < 0.05$ at 8 h), while there was no significant increase in Rad51 foci or any effect of NU7441 in DNA-PK-deficient M059 J cells. To confirm that this apparent dependency of IR-induced Rad51 focus on DNA-PK activity, we investigated the effect of NU7441 on Rad51 formation in NHEJ- and HR-proficient human colon cancer SW620 cells that we have previously used for studies of NU7441 chemo- and radio-sensitisation [11]. In these cells, we also observed an increase in radiation-induced Rad51 foci, which was inhibited by NU7441 (Fig. 4c). Both the increase in Rad51 and its inhibition by NU7441 were statistically significant ($P < 0.05$) in SW620 cells.

DNA-PKcs expression and activity in human tumours and surrogate normal tissues

To develop a pharmacodynamic biomarker to support clinical trials of DNA-PK inhibitors, it is necessary to demonstrate DNA-PK activation in tumour and surrogate normal tissue. We therefore determined whether pSer2056-DNA-PK could be used as an indicator of DNA-PK activation in the whole animal setting. We have previously used mice bearing SW620 human colorectal cancer xenografts for the pre-clinical evaluation of DNA-PK inhibitors [11] and therefore measured the induction of pSer2056-DNA-PK in SW620 xenografts in mice treated 1 and 24 h previously with a single dose of doxorubicin (20 mg/kg i.p.). There was a clear activation of DNA-PK in the tumours from the treated mice (Fig. 5a). For the surrogate normal tissue, we investigated the suitability of lymphocytes from healthy

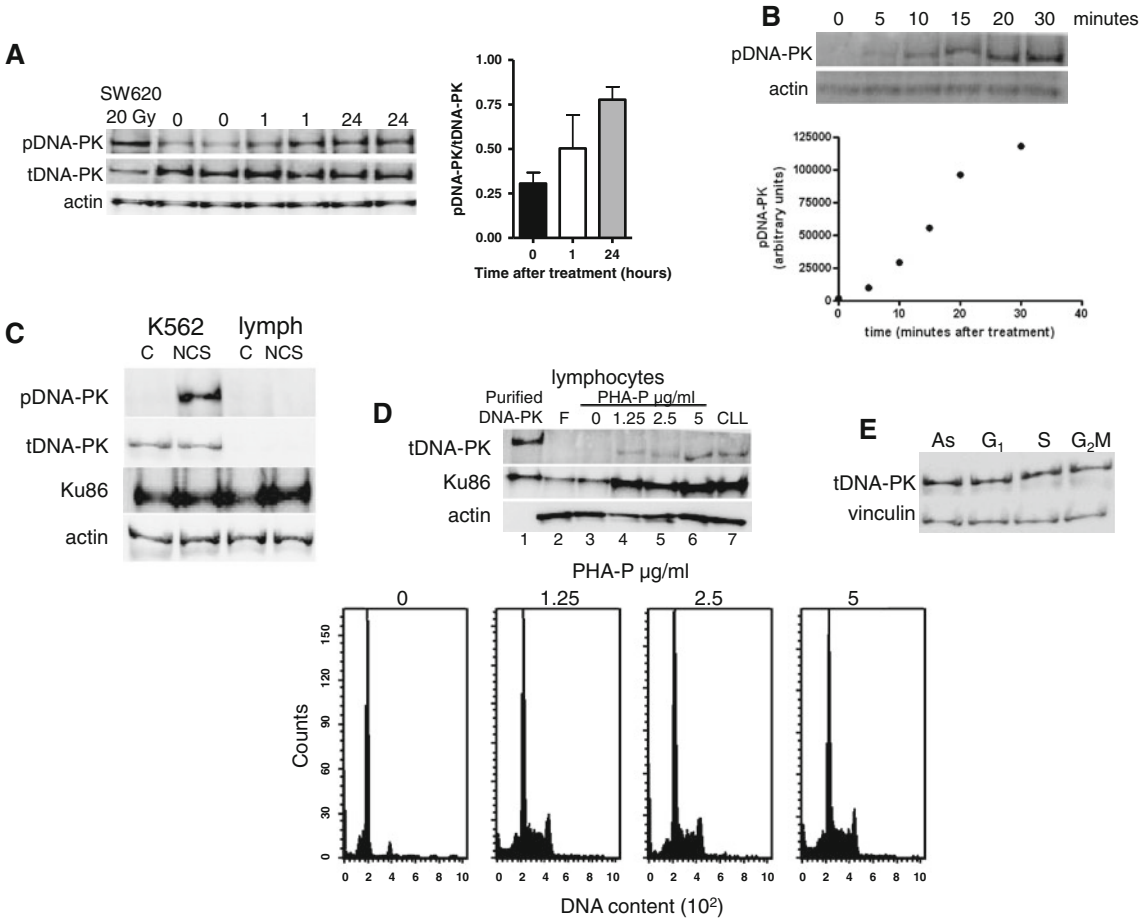

Fig. 5 DNA-PK activity is detected in human tumour xenografts and CLL cells, and the expression is not cell cycle phase dependent. **a** pSer2056 DNA-PK can be detected ex vivo in tumour samples from mice treated with doxorubicin. Tumours from two mice *per* time point were excised, ground, proteins extracted and 50 µg analysed. Shown are representative Western blots for phospho- and total DNA-PK, and the *graph* shows the data expressed as the mean pS2056-DNA-PK:total DNA-PK ratio ± SD. *Lane 1* is an extraction of SW620 cells exposed to 20 Gy in vitro as a positive control. **b** Accumulation of pSer2056-DNA-PKcs with continuous exposure to NCS. K562 cells were treated with 10 nM NCS, proteins extracted at different time points and 10 µg were analysed. Shown are representative Western blots from three independent experiments and the graph of phospho-DNA-PK levels during the first 30 min. **c** pSer2056-DNA-PK and total DNA-PK were undetectable in lymphocytes after DSB induction by NCS. Proteins extracted from K562 cells or lymphocytes prepared from NCS-treated fresh human blood were probed for pSer2056-DNA-PK. Shown is a representative Western blot from three independent experiments. Ku80 is a marker to confirm that nuclear proteins have been extracted. **d** DNA-PKcs is expressed in proliferating human lymphocytes and in a human CLL sample. 50 µg of protein extracted from resting/cycling lymphocytes and a CLL sample were analysed for total DNA-PK. Lane 1: purified DNA-PK holoenzyme, *lane 2* fresh lymphocytes, *lanes 3–6* 72 h-PHA-P-stimulated lymphocytes, *lane 7* CLL sample. Shown is a representative Western blot from three independent experiments. DNA *histograms* represent the distribution of cells in the different cell cycle phases for the cultivated lymphocyte samples. PHA-P: phytohemagglutinin-P stimulation for 72 h. **e** DNA-PK is equally expressed in all cell cycle phases. 20 µg of extracts from K562 cells separated into G_1, S and G_2M phases by centrifugal elutriation were analysed. *As* asynchronous

volunteers. To determine DNA-PK activity, DSBs had to be induced ex vivo. We considered that irradiation of the sample would be impractical in the clinical setting and therefore investigated the feasibility of using neocarzinostatin, an antibiotic that induces a high level of DSBs. Pilot studies with K562 cells demonstrated a rapid time-dependent activation of DNA-PK with a strong pSer2056-DNA-PK signal after 30-min exposure to 10 nM NCS (Fig. 5b). We therefore added 10 nM NCS to freshly isolated human blood 30 min prior to the isolation of the lymphocytes. Neither pSer2056-DNA-PK nor total DNA-PKcs could be detected in resting lymphocytes (Fig. 5c, d), but in lymphocytes that were stimulated to enter cell cycle with PHA-P (Fig. 5d), DNA-PKcs was clearly detectable. DNA-PKcs was also abundantly expressed in a CLL sample (Fig. 5d), confirming previous data [9]. Interestingly, Ku86, one of the two regulatory subunits of DNA-PK, was present in resting lymphocytes (Fig. 5b). As expected for an enzyme that can act at all phases of the cell cycle, we found no difference in the expression of DNA-PKcs at different phases of the cell cycle in K562 cells separated into G_1, S and G_2M phases by centrifugal elutriation (Fig. 5e).

Discussion

Cells lacking DNA-PK activity are hypersensitive to ionising radiation and topoisomerase II inhibitors; therefore, DNA-PK inhibition represents an attractive therapeutic manoeuvre to sensitise tumours to these anticancer treatments. We had previously shown that NU7441 selectively enhanced IR and etoposide sensitivity in DNA-PK-proficient but not DNA-PK-deficient Chinese hamster ovary cells [11]. Here, we extend these observations and demonstrate the DNA-PKcs dependence of potentiation using isogenically paired DNA-PK-proficient and DNA-PK-deficient human cancer cells.

We assessed the inhibition of DNA-PK by measuring the autophosphorylation site pSer2056, which is considered the most robust and specific target of DNA-PK activity. Together with the band for pSer2056-DNA-PK, we observed a series of non-specific bands occurring in both M059 J and M059-Fus-1 cells. Although the bands represented phosphorylation events, they did not appear to be DNA-PKcs degradation products and investigations with the ATM inhibitor KU-55933 suggested that they were related to ATM activity.

The catalytic domain of DNA-PK shares homology with that of PI3 K, and NU7441 is a structural analogue of the PI3 K inhibitor LY294002. In in vitro enzyme inhibition assays, NU7441 was approximately 350 times more active against DNA-PK than PI3 K [10]. However, in vitro activity and selectivity does not always predict cellular effects, and we have recently demonstrated that an ATP-competitive kinase inhibitor that was 50 times more selective for CDK2 than CDK1 in cell-free biochemical assays was equally active against both kinases in intact cells [22]. It was therefore important to determine the selectivity of NU7441 for DNA-PK in respect to PI3 K inhibition in whole cells. We calculated the cellular IC_{50} of NU7441 for DNA-PK inhibition to be 0.3 μM, i.e. about 30-fold less potent than in biochemical assays, which may reflect reduced uptake into cells or the different ATP concentration in cells (1–5 mM) compared with that used in the biochemical assay (18 μM). The NU7441 IC_{50} for PI3 K in cellular assays of AKT phosphorylation was 7 μM and therefore NU7441 is approximately 20-fold more selective for cellular DNA-PK than PI3 K. At the concentration of NU7441 used in subsequent studies (1 μM), PI3 K was not substantially inhibited in the cellular assay. The minimal effect on PI3 K clearly had no role in sensitisation to IR or doxorubicin, as NU7441 had no effect on the sensitivity of M059 J cells, which lack DNA-PKcs. M059 J cells were 18-fold more sensitive to doxorubicin and fourfold more sensitive to IR than M059-Fus-1 cells, which carry three or more copies of human chromosome 8, on which other genes for proteins related to DNA biology are located. The differential sensitivity of M059 J and M059-Fus-1 cells to genotoxic agents could therefore be due not only to DNA-PK but to other proteins encoded by genes on chromosome 8, for example NBS-1 and WRN. NBS-1 acts as an ATM stabiliser [23] and could enhance its function in M059-Fus-1 compared to M059 J cells, which express two different and less active forms (mutated and truncated) of ATM [13]. NU7441 enhanced IR cytotoxicity in M059-Fus-1 cells approximately twofold and caused a 3.5-fold sensitisation to doxorubicin. Treatment with NU7441 did not therefore make M059-Fus-1 cells as chemo- or radio-sensitive as M059 J cells (Table 1). Failure to increase sensitivity to the level observed in M059 J cells may be due to a number of factors: (1) NU7441 at 1 μM only inhibited DNA-PK by 70 and 100% inhibition may be needed for an equivalent effect or (2) other proteins encoded by genes on chromosome 8 might contribute to reduced doxorubicin sensitivity. Investigation into DSB repair by measuring γ-H2AX foci revealed that M059-Fus-1 cells largely repaired IR-induced DSB within 24 h. Kinetics of γ-H2AX foci dissolution in M059-Fus-1 cells were somewhat slower than we had observed previously in SW620 cells [11], reflecting variation of repair rates in different cell types. In M059-Fus-1 cells, NU7441 retarded both the peak in γH2AX focus formation and their disappearance, with at least 32% of the foci remaining at 24 h. Presumably, the change in focus kinetics reflects a slowing of the rate of γH2AX focus formation due to DNA-PK-mediated phosphorylation of this protein coupled with the increased persistence of the breaks and ATM activation (Fig. 1b). The high basal levels of γH2AX foci in M059 J cells may be due to the activity of alternative kinases; as microfoci have previously been described that occur in the absence of DNA damage and do not co-localise with other DNA repair enzymes [24, 25].

We postulated that when DNA-PK was defective or inhibited, cells would be more reliant on HR for DNA DSB repair. This hypothesis is supported by published observation of higher levels of Rad51 in DNA-PK defective cells [26]. Surprisingly, we found not only that M059 J cells had lower basal Rad51 levels, with no induction by IR, but that IR-induced Rad51 foci were reduced by NU7441 in both M059-Fus-1 and SW620 cells. These observations led us to formulate three hypotheses: (1) NU7441 inhibits a kinase in the HR pathway, (2) DNA-PK participates in HR or (3) in the presence of NU7441, DNA-PK remains bound to DSB, thus obstructing the access of other repair proteins. The first hypothesis is unlikely, due to the lack of activity of NU7441 against a panel of kinases at the concentrations used in this study [10], but cannot be totally excluded as an exhaustive investigation into the effects of NU7441 on all HR-associated enzymes has not been conducted. The second hypothesis is consistent with the failure of IR to increase Rad51 foci in M059 J cells; however, we cannot establish whether this failure was due to lack of DNA-PK or lower ATM activity. Previous data [27] showed that

DNA-PK and PARP-1 co-operated in DSB resolution, and the same relationship could exist between DNA-PK and ATM for HR function. The third hypothesis is supported by data from a recent report in which a recombinant DNA-PK lacking phospho-residues (thereby mimicking NU7441-inhibited DNA-PK) was found to be more tightly bound to DNA [28], and other studies suggesting that DNA-PK inhibition obstructs the access of PARP-1 to DNA ends [29]. Although outside the scope of the current study, these observations clearly warrant further investigations using the complementary approaches of genetic and small molecule manipulation of repair pathways.

We were unable to detect DNA-PK in normal human PBMCs, a potential surrogate tissue for biomarker studies. The lack of DNA-PK may reflect the quiescent nature of these terminally differentiated cells, although studies in K562 cells failed to show any cell cycle dependence of DNA-PK expression. Previous studies show that DNA-PK is abundant in CLL [9] and lung cancer cells [30], and therefore, the most appropriate samples for PD biomarker monitoring may be the tumour itself. Clearly, further work on appropriate biomarkers is warranted, but it may be most informative to conduct phase 0/I studies in leukaemia and lung cancer patients.

Acknowledgments We gratefully acknowledge the financial support of CR UK (NJC, CC and DRN) and AstraZeneca (MT and JMM), Newcastle Cancer Centre-Medicinal Chemistry, Newcastle University, for providing NU7441 and ZSTK474 and Dr GCM Smith, AstraZeneca for providing KU55933.

References

1. Lisby M, Rothstein R (2009) Choreography of recombination proteins during the DNA damage response. DNA Repair (Amst) 8(9):1068–1076
2. Uematsu N et al (2007) Autophosphorylation of DNA-PKCS regulates its dynamics at DNA double-strand breaks. J Cell Biol 177(2):219–229
3. Hartlerode AJ, Scully R (2009) Mechanisms of double-strand break repair in somatic mammalian cells. Biochem J 423(2):157–168
4. Stavnezer J, Guikema JE, Schrader CE (2008) Mechanism and regulation of class switch recombination. Annu Rev Immunol 26:261–292
5. Bosma MJ, Carroll AM (1991) The SCID mouse mutant: definition, characterization, and potential uses. Annu Rev Immunol 9:323–350
6. Smith GC, Jackson SP (1999) The DNA-dependent protein kinase. Genes Dev 13(8):916–934
7. Arlander SJ et al (2008) DNA protein kinase-dependent G2 checkpoint revealed following knockdown of ataxia-telangiectasia mutated in human mammary epithelial cells. Cancer Res 68(1):89–97
8. Muller C et al (1998) DNA-Dependent protein kinase activity correlates with clinical and in vitro sensitivity of chronic lymphocytic leukemia lymphocytes to nitrogen mustards. Blood 92(7):2213–2219
9. Willmore E et al (2008) DNA-dependent protein kinase is a therapeutic target and an indicator of poor prognosis in B-cell chronic lymphocytic leukemia. Clin Cancer Res 14(12):3984–3992
10. Leahy JJ et al (2004) Identification of a highly potent and selective DNA-dependent protein kinase (DNA-PK) inhibitor (NU7441) by screening of chromenone libraries. Bioorg Med Chem Lett 14(24):6083–6087
11. Zhao Y et al (2006) Preclinical evaluation of a potent novel DNA-dependent protein kinase inhibitor NU7441. Cancer Res 66(10):5354–5362
12. Shinichi Y, Koshimizu I, Yoshimi H, Matsuno T, Watanabe T, Tsuchida Y, Saitho K (2007) Treatment of prostate cancer, melanoma or hepatic cancer. Zenyaku Kogyo Kabushiki Kaisha, USA
13. Tsuchida R et al (2002) Detection of ATM gene mutation in human glioma cell line M059 J by a rapid frameshift/stop codon assay in yeast. Radiat Res 158(2):195–201
14. Rogakou EP et al (1998) DNA double-stranded breaks induce histone H2AX phosphorylation on serine 139. J Biol Chem 273(10):5858–5868
15. Willmore E, de Caux S, Sunter NJ, Tilby MJ, Jackson GH, Austin CA, Durkacz BW (2004) A novel DNA-dependent protein kinase inhibitor, NU7026 potentiates the cytotoxicity of topoisomerase II poisons used in the treatment of leukemia. Blood 103(12):7
16. Zhao H, Piwnica-Worms H (2001) ATR-mediated checkpoint pathways regulate phosphorylation and activation of human Chk1. Mol Cell Biol 21:10
17. Bakkenist CJ, Kastan MB (2002) DNA damage activates ATM through intermolecular autophosphorylation and dimer dissociation. Nature 421:8
18. Datta J et al (2009) A new class of quinoline-based DNA hypomethylating agents reactivates tumor suppressor genes by blocking DNA methyltransferase 1 activity and inducing its degradation. Cancer Res 69(10):4277–4285
19. Terme JM et al (2009) TGF-beta induces degradation of TAL1/SCL by the ubiquitin-proteasome pathway through AKT-mediated phosphorylation. Blood 113(26):6695–6698
20. Hickson I et al (2004) Identification and characterization of a novel and specific inhibitor of the ataxia-telangiectasia mutated kinase ATM. Cancer Res 64(24):9152–9159
21. Grimberg A (2003) Mechanisms by which IGF-I may promote cancer. Cancer Biol Ther 2(6):630–635
22. Johnson N et al (2009) Pre-clinical evaluation of cyclin-dependent kinase 2 and 1 inhibition in anti-estrogen-sensitive and resistant breast cancer cells. Br J Cancer 102(2):342–350
23. Lee JH, Paull TT (2007) Activation and regulation of ATM kinase activity in response to DNA double-strand breaks. Oncogene 26(56):7741–7748
24. McManus KJ, Hendzel MJ (2005) ATM-dependent DNA damage-independent mitotic phosphorylation of H2AX in normally growing mammalian cells. Mol Biol Cell 16(10):13
25. Marti TM, Hefner E, Feeney L, Natale V, Cleaver JE (2006) H2AX phosphorylation within the G1 phase after UV irradiation depends on nucleotide excision repair and not DNA double-strand breaks. Proc Natl Acad Sci USA 103(26):6
26. Shrivastav M et al (2009) DNA-PKcs and ATM co-regulate DNA double-strand break repair. DNA Repair (Amst) 8(8):920–929
27. Mitchell J, Smith GC, Curtin NJ (2009) Poly(ADP-Ribose) polymerase-1 and DNA-dependent protein kinase have equivalent roles in double strand break repair following ionizing radiation. Int J Radiat Oncol Biol Phys 75(5):1520–1527
28. Hammel M et al (2010) Ku and DNA-dependent protein kinase (DNA-Pk) dynamic conformations and assembly regulate DNA binding and the initial nonhomologous end joining complex. J Biol Chem 285(2):1414–1423
29. Veuger SJ et al (2004) Effects of novel inhibitors of poly(ADP-ribose) polymerase-1 and the DNA-dependent protein kinase on enzyme activities and DNA repair. Oncogene 23(44):7322–7329
30. Zhuang HQ et al (2009) Radiosensitizing effects of gefitinib at different administration times in vitro. Cancer Sci 100(8):1520–1525